Int. J. Heat Mass Transfer. Vol. 30, No. 7, pp. 1319–1329, 1987
Printed in Great Britain

0017–9310/87 $3.00 + 0.00

Instabilities in a double-diffusive thermosyphon

YORAM ZVIRIN
Faculty of Mechanical Engineering, Technion—Israel Institute of Technology, Haifa 3200, Israel

(*Received* 27 *June* 1986 *and in final form* 30 *October* 1986)

Abstract—The steady state and the stability behaviour of a double-diffusive natural circulation loop are investigated theoretically. The fluid in the thermosyphon consisting of two vertical channels is subjected to both temperature and salinity gradients. The governing equations of continuity, momentum, energy and mass diffusion are written based on a one-dimensional model for laminar flow. The steady-state solutions include the trivial 'conductive' one of no flow in the loop, $v = 0$, and 'convective' flow solutions when the thermal Rayleigh number, R_T, exceeds a critical value, R_{Tc}, which depends on the saline Rayleigh number, R_S, and the inverse Lewis number, q. In a certain range of system parameters double 'convective solutions' are obtained. The results of linear stability analysis show that the one with lower v is always unstable and all the other steady flow solutions are stable. The stability chart in the plane R_S–R_T, derived by this analysis, also includes a description of instabilities associated with the onset of motion from rest. The marginal stability boundaries include the monotonic marginal stability lines (MMSL) $R_T = 6 + qR_S$, and oscillatory ones (OMSL) which depend also on the Prandtl number and bifurcate from the MMSL. An interesting phenomenon, exhibited from the solution, is that the OMSL intersects the line R_{Tc}, representing the critical conditions for existence of steady flow solutions.

1. INTRODUCTION

THE FIELDS of natural circulation loops (thermosyphons) and double-diffusive processes have gained increased interest in the last two decades. Flows with both phenomena appear in energy conversion systems and in geophysical processes, and exhibit various kinds of instabilities, e.g. refs. [1–5]. Although several thermosyphons involve diffusion of both heat and mass (i.e. in solar energy systems and in nuclear reactor cooling loops), not much work has been done, to date, on double-diffusive processes in natural convection loops. The only available studies are those of Siegmann and Rubenfeld [6, 7], Hart [8] and Zvirin [9].

Three distinct types of instabilities have been found (experimentally and theoretically) in thermosyphons, except for the local formation of 'classical' Rayleigh–Bénard closed cells:

(a) the onset of flow around the loop;
(b) instability of a steady loop flow;
(c) multiple steady-state solutions, i.e. meta-stable equilibrium states.

All three types, associated with global flow around the loops, have been discussed in ref. [10], including the controversy in the literature about critical conditions for the onset of motion. It is noted that natural circulation loops exhibit, in addition, the 'peculiar' chaotic behaviour of transient flows [8, 11–13].

Siegmann and Rubenfeld [6] obtained a critical condition for the onset of motion in a toroidal loop with temperature and concentration gradients. In their analysis, however, they neglected the thermal and saline diffusivities and defined Rayleigh numbers based on heat and mass convection coefficients between the fluid in the loop and the surroundings. Hart [8] studied the same system with the inclusion of diffusion and thermal diffusion (Soret effect) but neglecting, again, thermal conduction. He also found chaotic transient behaviour which was previously discovered in loops with temperature gradients only [11–13]. Critical conditions were derived in refs. [12–14] for initiation of flows in thermosyphons with a single gradient of temperature, using a similar approach.

The thermal and saline diffusivities must be accounted for in problems of flow initiation from a rest state, where the convection slowly develops from zero. Moreover, the first two effects are the sole mechanisms for heat and mass transfer in an insulated channel just prior to the onset of motion [15]. Zvirin has derived correct critical conditions for the stability margins of vertical single-channel and multi-channel thermosyphons [10, 16] and a toroidal loop [17], taking into consideration these diffusivities. The results of the latter indicate, indeed, that the previous analyses [6–8, 12–14] may be regarded as approximations for large values of the Rayleigh and Biot numbers. Zvirin [9] investigated a double-diffusive vertical thermosyphon, and found multiple steady-state solutions. His study did not include stability analyses of the rest state and the steady flows.

The present work is a theoretical investigation of the stability of a vertical loop with double-diffusive processes. The characteristic stability equations are derived from the continuity, momentum, energy and salinity conservation equations, by the linear stability analysis. Critical conditions are obtained for the onset of motion from the rest state, and the stability margins of the multiple steady solutions is determined.

NOMENCLATURE

- a radius of pipe
- B function of the steady velocity, equation (15)
- F function of v and σ, equation (25a)
- f friction coefficient
- G function of v, q and σ, equation (25b)
- g acceleration of gravity
- K_S solute diffusivity
- K_T thermal diffusivity
- L height of the loop
- M steady-state temperature distribution, equation (13a)
- N steady-state salinity distribution, equation (13b)
- P modified Prandtl number, equation (12)
- q inverse Lewis number, equation (12)
- R_S modified saline Rayleigh number, equation (12)
- R_T modified thermal Rayleigh number, equation (12)
- S salinity
- T temperature
- t dimensionless time, equation (7)
- u velocity perturbation
- V velocity
- v dimensionless velocity, equation (7)
- w oscillation frequency, Im (σ)
- Y complex function, equations (24) and (27)
- Z vertical coordinate
- z dimensionless vertical coordinate, equation (7).

Greek symbols

- β_S saline expansion coefficient
- β_T thermal expansion coefficient
- $\gamma_{1,2}$ parameters, equation (22c)
- $\delta_{1,2}$ parameters, equation (23c)
- θ dimensionless temperature, equation (7)
- λ parameter, equation (26c)
- μ parameter, equation (26c)
- ν kinematic viscosity
- ρ density
- σ stability parameter
- τ time
- ϕ dimensionless salinity, equation (7)
- ψ temperature perturbation
- ω salinity perturbation.

Subscripts

- c critical (Rayleigh number)
- D lower container
- S related to salinity
- T related to temperature
- U upper container
- 1, 2 channels with upward and downward flows (except for the parameters $\gamma_{1,2}$, $\delta_{1,2}$).

Superscripts

- * bifurcation of monotonic and oscillatory marginal stability lines
- $\bar{()}$ steady state.

2. THE THEORETICAL MODEL AND GOVERNING EQUATIONS

Figure 1 describes schematically the loop analyzed here: two insulated† channels connecting two large containers, with constant temperatures and salinities T_D, S_D and T_U, S_U. The density of the fluid in the loop depends on both temperature and salinity

$$\rho = \rho_U[1-\beta_T(T-T_U)+\beta_S(S-S_U)] \quad (1)$$

where β_T and β_S are the thermal and saline expansion coefficients. The Boussinesq approximation is used, i.e. the density and all the other fluid properties are taken as constants in the governing equations except for the body force term in the momentum equation.

It is assumed that the effects of surface tension and local pressure drops at the connections between the channels and the containers can be neglected, i.e. the pipes are wide and long enough. The length of the channel also enables the assumption of constant boundary conditions. This requirement might be hard to realize in an experimental system for the investigation of stability and oscillations of the steady flow unless the pipes are long and the connections are carefully designed. However, the main interest in the present study is the conditions associated with the

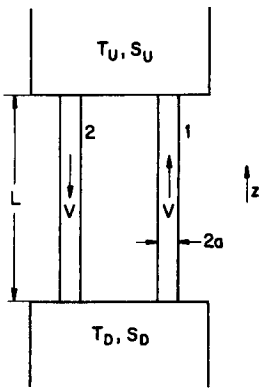

FIG. 1. A scheme of the vertical thermosyphon with double-diffusive processes.

† The effects of heat fluxes through the side walls are discussed at the end of Section 4.

onset of motion from rest. For this the constant boundary conditions can easily be arranged. Moreover, laminar flow can be considered, and according to the results of refs. [18, 19] we can adopt a one-dimensional model, with the friction coefficient taken as that for forced flow, i.e. $f = 16/Re = 16\nu/2aV$.

It follows from these assumptions and from the continuity equation that the velocity in the loop is a function of the time, τ, only having the same magnitude in the two branches

$$V_1(\tau) = V_2(\tau) = V(\tau) \tag{2}$$

where the subscripts 1, 2 denote channels with upward and downward flows, respectively.

The momentum equation is integrated around the loop to eliminate the pressure terms, as usual in treatments of thermosyphons, cf. refs. [1, 2, 8–10]

$$\frac{dV}{d\tau} = -\frac{g}{2L\rho_U}\oint \rho\, dZ - \frac{8\nu}{a^2}V \tag{3}$$

where Z is the vertical coordinate and the above-mentioned friction correlation has been used in the last term of equation (3). The energy and diffusion equations for the temperature and salinity distributions are

$$\frac{\partial T}{\partial \tau} \pm V\frac{\partial T}{\partial Z} = K_T\frac{\partial^2 T}{\partial Z^2} \tag{4}$$

$+$ upward flow (1)
$-$ downward flow (2)

$$\frac{\partial S}{\partial \tau} \pm V\frac{\partial S}{\partial Z} = K_S\frac{\partial^2 S}{\partial Z^2} \tag{5}$$

where K_T and K_S are the thermal and saline diffusivities. The boundary conditions are

$$T = T_D, \quad S = S_D, \quad \text{at} \quad Z = 0 \tag{6a}$$

$$T = T_U, \quad S = S_U, \quad \text{at} \quad Z = L. \tag{6b}$$

The following transformations are used to define the dimensionless variables:

$$z \equiv Z/L, \quad v \equiv LV/K_T, \quad t \equiv K_T\tau/L^2$$
$$\theta \equiv (T-T_U)/(T_D-T_U), \quad \phi \equiv (S-S_U)/(S_D-S_U). \tag{7}$$

The governing equations (3)–(5) and boundary conditions (6) are transformed to dimensionless form

$$\frac{1}{P}\frac{\partial v}{\partial t} = R_T\int_0^1 (\theta_1-\theta_2)\,dz - R_S\int_0^1 (\phi_1-\phi_2)\,dz - v \tag{8}$$

$$\frac{\partial \theta}{\partial t} \pm v\frac{\partial \theta}{\partial z} = \frac{\partial^2\theta}{\partial z^2} \tag{9}$$

$+$ upward flow (1)
$-$ downward flow (2)

$$\frac{\partial \phi}{\partial t} \pm v\frac{\partial \phi}{\partial z} = \frac{1}{q}\frac{\partial^2\phi}{\partial z^2} \tag{10}$$

$$\theta = 1, \quad \phi = 1 \quad \text{at} \quad z = 0 \tag{11a}$$

$$\theta = 0, \quad \phi = 0 \quad \text{at} \quad z = 1. \tag{11b}$$

This system of governing equations and boundary conditions includes the four dimensionless parameters

$$R_T \equiv \frac{g\beta_T(T_D-T_U)La^2}{16\nu K_T} \quad \text{thermal Rayleigh number}$$

$$R_S \equiv \frac{g\beta_S(S_D-S_U)La^2}{16\nu K_T} \quad \text{saline Rayleigh number} \tag{12}$$

$$P \equiv 8\left(\frac{L}{a}\right)^2\frac{K_T}{\nu} \quad \text{modified Prandtl number}$$

$$q \equiv K_T/K_S \quad \text{inverse Lewis number.}$$

The thermal Rayleigh number is destabilizing (tends to create a loop flow) while the saline one is stabilizing.

3. STEADY-STATE SOLUTIONS

The steady-state solution, derived by Zvirin [9], is briefly reviewed here because it is needed for the stability analysis in the next section. Also, the results of ref. [9] are extended here: additional information is presented, including discussions of new features of the solution.

At steady state all the time derivatives in equations (8)–(10) vanish. As can be seen, the solution depends, then, only on the Rayleigh and Lewis numbers and not on the Prandtl number. The solution procedure is similar to other analytical solutions of free convection loops, cf. refs. [1, 2, 9, 10]: at the first stage, the energy and diffusion equations (9) and (10) are solved, with boundary conditions (11), for the temperature and salinity distributions in terms of the constant velocity, v, which is yet an unknown parameter

$$\theta_1 = M(z;v) = \frac{e^{vz}-e^{v}}{1-e^{v}}, \quad \theta_2 = M(z;-v) \tag{13a}$$

$$\phi_1 = N(z;qv) = \frac{e^{qvz}-e^{qv}}{1-e^{qv}}, \quad \phi_2 = N(z;-qv). \tag{13b}$$

These distributions are introduced now into the momentum equation (8), and the integrations are performed. The result is the following algebraic equation for v:

$$R_T\left(\frac{e^{v}+1}{e^{v}-1}-\frac{2}{v}\right) - R_S\left(\frac{e^{qv}+1}{e^{qv}-1}-\frac{2}{qv}\right) = v. \tag{14}$$

In general, this equation must be solved numerically to obtain $v(R_T, R_S, q)$. The solution procedure is quite simple, however, because equation (14) can be rearranged such as to find $R_T(v; R_S, q)$ by a straightforward computation. The equation has a trivial, 'conductive' solution, $v = 0$, discussed below. Figures 2 and 3 show the results for the steady velocity of the 'convective' solution, v, as a function of the thermal

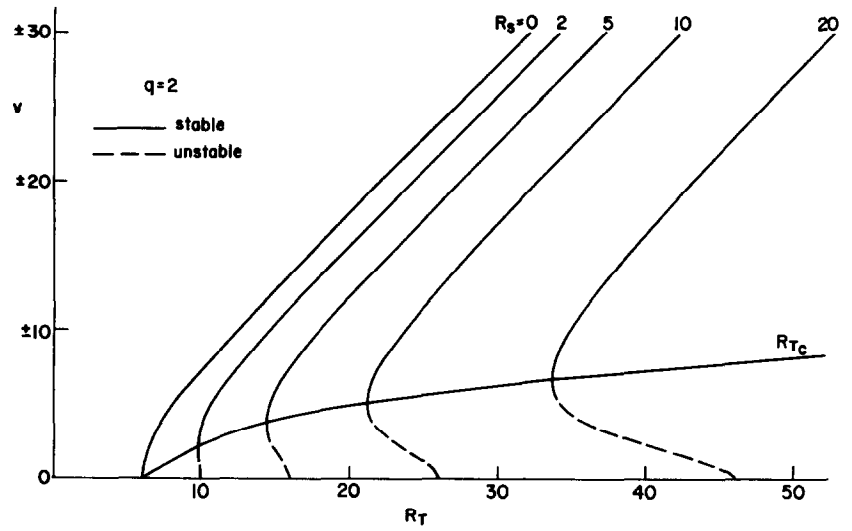

FIG. 2. The dimensionless steady-state velocity, v ('convective solution'), as a function of the thermal Rayleigh number, R_T, for various values of the saline Rayleigh number, R_S. The inverse Lewis number is $q = 2$.

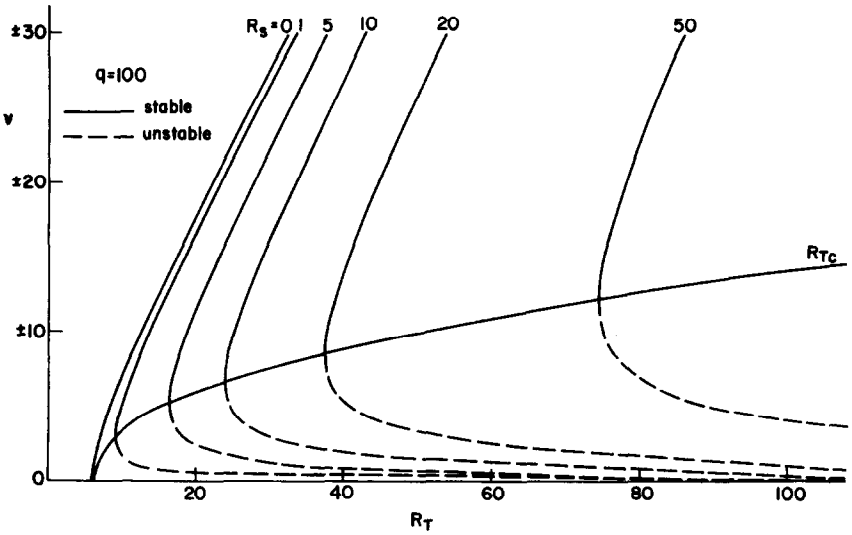

FIG. 3. The dimensionless steady-state velocity, v ('convective solution'), as a function of the thermal Rayleigh number, R_T, for various values of the saline Rayleigh number, R_S. The inverse Lewis number is $q = 100$.

Rayleigh number, R_T, with the saline Rayleigh number, R_S, as a parameter, and for two values of the inverse Lewis number, $q = 2$, 100. The most interesting feature of the steady-state flow is the existence of double solutions for $q > 1$ and $R_S > 0$. It is noted that multiple steady-state solutions have been previously discovered in thermosyphons [20–23] and also in double-diffusive loops [6–9]. The occurrence of multiple steady flows is caused by the non-monotonic dependence of the buoyancy forces (the integral terms in the momentum equation (8)) on the velocity, as explained by ref. [21].

The lines R_{Tc} in Figs. 2 and 3 are the loci of the minimal values of R_T on the curves for v. They can be obtained formally from equation (14) in the following way. The equation is rearranged, as mentioned above, to read $R_T = R_T(v; R_S, q)$. R_{Tc} is found from the condition $dR_T/dv = 0$, which leads to

$$\frac{1}{B^2}\left\{\left(\frac{e^v+1}{e^v-1}-\frac{2}{v}\right)\left[1+R_S\left(\frac{-2qe^{qv}}{(e^{qv}-1)^2}+\frac{2}{qv^2}\right)\right]-\left[v+R_S\left(\frac{e^{qv}+1}{e^{qv}-1}-\frac{2}{qv}\right)\right]\left[\frac{-2e^v}{(e^v-1)^2}+\frac{2}{v^2}\right]\right\}=0 \tag{15}$$

where

$$B \equiv \frac{e^v+1}{e^v-1}-\frac{2}{v}.$$

This equation can be solved, in principle, for

$v_c = v_c(R_S, q)$, and the result introduced back into equation (14) to obtain $R_{Tc}(R_c, q)$.

For every value of q and R_S, there does not exist a steady loop flow when $R_T < R_{Tc}$. These critical lines for the existence of steady states are shown in the stability charts on Figs. 4–6 as R_{Tc} (R_S) for various values of q.

Reference [9] includes analytical approximations derived asymptotically from equation (14) for small and large values of the velocity v. The former also yields the limiting condition for $v = 0$: $R_T = 6 + qR_S$. The results of ref. [10] for a thermosyphon with a single gradient of temperature are obtained from the present solution by introducing $R_S = 0$. No double solutions such as illustrated in Figs. 2 and 3 appear in this case.

Let us examine now the rest state of no flow in the loop. As discussed in ref. [9], the 'trivial solution', $v = 0$, is related to the symmetry of the system: in a non-symmetric loop a flow would always be established upon activation of the driving mechanism (the heat source). In the loop treated here (Fig. 1), there is no preferred direction thus for any positive solution, v, the mirror image flow, $-v$, is also a solution. This is a further multiplicity of the steady-state solution.

The temperature and salinity distributions are obtained from expressions (13) by inserting the steady-state velocity, v (the solution of equation (14)). For the rest case, we can introduce $v = 0$ into equations (9)–(11), and solve them to get

$$\bar{\theta}_{1,2} = \bar{\phi}_{1,2} = 1 - z, \quad v = 0. \tag{16}$$

These profiles are also obtained by expanding equations (13) for $v \to 0$. The momentum equation (8) is identically satisfied by the solution (16) for the rest state. This solution for the no-flow situation is also referred to as the 'conductive solution', cf. [6].

The conductive solution would naturally be established when the system parameters are such that the rest state is stable. In an experimental system it is possible to obtain the no-flow solutions for unstable states by blocking the flow, using a conductive membrane. This was done [24] in a test with a completely stagnant channel of a multiple-loop system.

We summarize now the results for the steady-state solutions for the double-diffusive thermosyphon (see also Figs. 2–6):

(a) A trivial 'conductive' solution, $v = 0$, always exists: for all values of R_T, R_S and q.

(b) No flow solution for all q and R_S when $R_T < R_{Tc}$. R_{Tc} is determined from equation (15).

(c) Double steady flow solutions for all $q > 1$, when $R_S > 0$, in the range $R_{Tc} < R_T \leqslant 6 + qR_S$ (the region between these two lines in Figs. 4–6).

(d) A single steady flow solution for all q and R_S when $R_T > 6 + qR_S$.

It is noted, again, that all flow solutions are pairs of

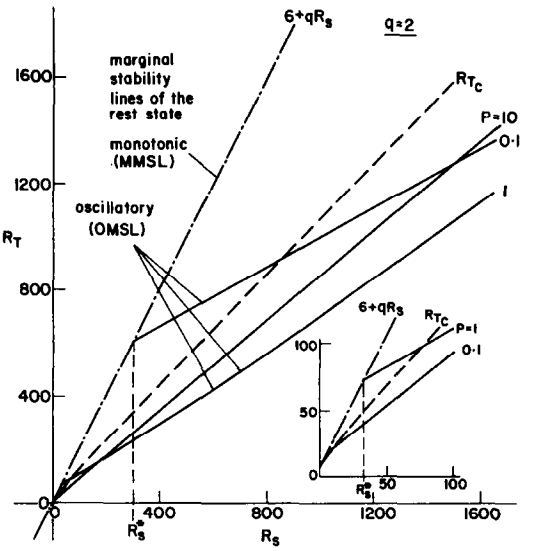

FIG. 4. The stability chart in the Rayleigh numbers plane, R_S–R_T, for the inverse Lewis number, $q = 2$.

v and $-v$. For example, case (c) above includes five different solutions: the two pairs and the rest state $v = 0$. The term 'exists' means, here, a solution obtained from the governing steady-state equations (8)–(11). Actual 'existence' depends on the *stability* of the solutions, analyzed and discussed in the next section.

4. STABILITY ANALYSIS

4.1. *The characteristic equations*

The method of linear stability analysis is employed for the investigation of the various steady-state solutions derived in the previous section. We start with the formulation for the steady flow solutions, and write the time-dependent velocity, temperature and salinity as

$$v = \bar{v} + u e^{\sigma t}, \quad \theta = \bar{\theta} + \psi(z) e^{\sigma t}, \quad \phi = \bar{\phi} + \omega(z) e^{\sigma t} \tag{17}$$

where $\bar{v}$, $\bar{\theta}$ and $\bar{\phi}$ now denote the steady-state values: $\bar{v}$ is the solution of equation (14) (results appear in Figs. 2 and 3) and $\bar{\theta}$ and $\bar{\phi}$ are obtained by introducing $\bar{v}$ into equations (13). The perturbations u, ψ and ω are considered small. For the stability study of the onset of motion from rest, $\bar{v} = 0$ and $\bar{\theta}$ and $\bar{\phi}$ are given in equation (16). The stability parameter, σ, in equation (17) may generally be complex, and the state is unstable when $\mathrm{Re}(\sigma) > 0$, while $\mathrm{Re}(\sigma) = 0$ yields the marginal stability.

Expressions (17) are introduced into the time-dependent governing equations and boundary conditions (8)–(11). The steady-state terms cancel identically and second-order products such as $u\psi$ and $u\omega$ are neglected. Thus the momentum, energy and diffusion perturbation equations are obtained

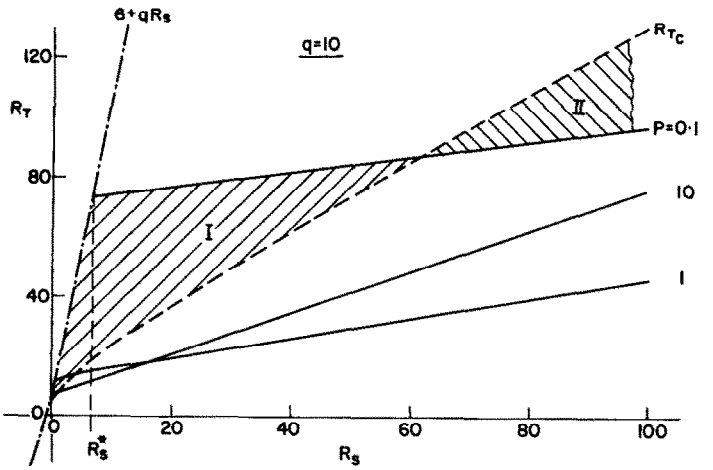

FIG. 5. The stability chart in the Rayleigh numbers plane, R_S–R_T, for the inverse Lewis number, $q = 10$.

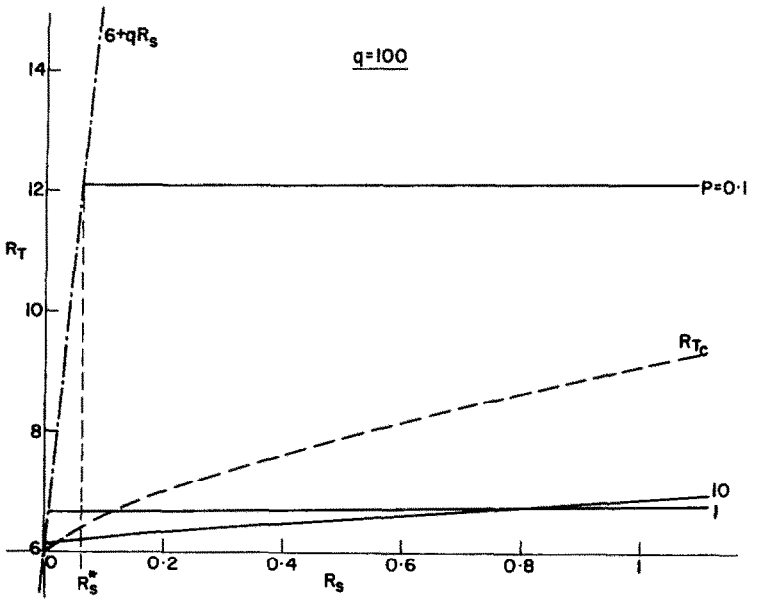

FIG. 6. The stability chart in the Rayleigh numbers plane, R_S–R_T, for the inverse Lewis number, $q = 100$.

$$u\left(\frac{\sigma}{P}+1\right) = R_T\int_0^1 (\psi_1-\psi_2)\,dz - R_S\int_0^1 (\omega_1-\omega_2)\,dz \quad (18)$$

$$\frac{d^2\psi}{dz^2} \mp \bar{v}\frac{d\psi}{dz} - \sigma\psi = \pm u\frac{d\bar{\theta}}{dz} \quad (19)$$

+ upward steady flow (1)
− downward steady flow (2)

$$\frac{1}{q}\frac{d^2\omega}{dz^2} \mp \bar{v}\frac{d\omega}{dz} - \sigma\omega = \pm u\frac{d\bar{\phi}}{dz} \quad (20)$$

with the boundary conditions

$$\psi_1 = \psi_2 = \omega_1 = \omega_2 = 0 \quad \text{at} \quad z = 0, 1. \quad (21)$$

The solution procedure is similar to that of the steady-state problem; equations (19)–(21) are solved, first, for the temperature and salinity perturbations ψ and ω in terms of the velocity perturbation, u, which is an unknown constant. The derivatives $d\bar{\theta}/dz$ and $d\bar{\phi}/dz$ are obtained by differentiation of equations (13). The following solutions resemble those of ref. [16] for a thermosyphon with a temperature gradient only, and for brevity we write v for the steady-state velocity (instead of $\bar{v}$)

$$\psi_1 = \frac{u}{\sigma}\frac{v}{1-e^v}\left\{\frac{1}{e^{\gamma_1}-e^{\gamma_2}}[(e^v-e^{\gamma_2})e^{\gamma_1 z} + (e^{\gamma_1}-e^v)e^{\gamma_2 z}] - e^{vz}\right\} \quad (22a)$$

$$\psi_2 = \frac{u}{\sigma}\frac{v}{1-e^{-v}}\left\{\frac{1}{e^{-\gamma_2}-e^{-\gamma_1}}[(e^{-v}-e^{-\gamma_1})e^{-\gamma_2 z} + (e^{-\gamma_2}-e^{-v})e^{-\gamma_1 z}] - e^{-vz}\right\} \quad (22b)$$

$$\gamma_{1,2} = \tfrac{1}{2}[v \pm \sqrt{(v^2+4\sigma)}] \quad (22c)$$

$$\omega_1 = \frac{u}{\sigma}\frac{qv}{1-e^{qv}}\left\{\frac{1}{e^{\delta_1}-e^{\delta_2}}[(e^{qv}-e^{\delta_2})e^{\delta_1 z} + (e^{\delta_1}-e^{qv})e^{\delta_2 z}] - e^{qvz}\right\} \quad (23a)$$

$$\omega_2 = \frac{u}{\sigma}\frac{qv}{1-e^{qv}}\left\{\frac{1}{e^{-\delta_2}-e^{-\delta_1}}[(e^{-qv}-e^{-\delta_1})e^{-\delta_2 z} + (e^{-\delta_2}-e^{-qv})e^{-\delta_1 z}] - e^{-qvz}\right\} \quad (23b)$$

$$\delta_{1,2} = \frac{q}{2}[v \pm \sqrt{(v^2+4\sigma/q)}]. \quad (23c)$$

These temperature and salinity distributions are now introduced into the perturbation momentum equation (18). The constant u cancels out, and after the integrations are performed we get the characteristic equation for the stability parameter σ

$$Y(\sigma) = \frac{\sigma}{P} + 1 - 2(R_T F - R_S G) = 0 \quad (24)$$

where

$$F \equiv \frac{1}{\sigma}\left\{\frac{v}{1-e^{v}}\frac{1}{e^{\gamma_1}-e^{\gamma_2}}\left[\frac{1}{\gamma_1}(e^{v}-e^{\gamma_2})(e^{\gamma_1}-1) + \frac{1}{\gamma_2}(e^{\gamma_1}-e^{v})(e^{\gamma_2}-1)\right] + 1\right\} \quad (25a)$$

$$G \equiv \frac{1}{\sigma}\left\{\frac{qv}{1-e^{qv}}\frac{1}{e^{\delta_1}-e^{\delta_2}}\left[\frac{1}{\delta_1}(e^{qv}-e^{\delta_2})(e^{\delta_1}-1) + \frac{1}{\delta_2}(e^{\delta_1}-e^{qv})(e^{\delta_2}-1)\right] + 1\right\}. \quad (25b)$$

For the investigation of the stability associated with the onset of motion from rest, we introduce into equations (19) and (20) $\bar{v} = 0$ and the derivatives of $d\bar{\theta}/dz$, $d\bar{\phi}/dz$ from equation (16). The solutions for the temperature and salinity perturbations are presented in a simpler form compared to [10, 16]

$$\psi_1 = -\psi_2 = \frac{u}{\sigma}\left\{1 - \frac{1}{e^{\lambda}+1}[e^{\lambda z} + e^{\lambda(1-z)}]\right\} \quad (26a)$$

$$\bar{v} = 0$$

$$\omega_1 = -\omega_2 = \frac{u}{\sigma}\left\{1 - \frac{1}{e^{\mu}+1}[e^{\mu z} + e^{\mu(1-z)}]\right\} \quad (26b)$$

$$\lambda \equiv \sqrt{\sigma}, \quad \mu \equiv \sqrt{(q\sigma)}. \quad (26c)$$

Introducing these expressions into equation (18) and carrying out the integration we obtain the characteristic equation

$$Y_0(\sigma) = \frac{\sigma}{P} + 1 - \frac{2}{\sigma}\left\{R_T\left[1 - \frac{2(e^{\lambda}-1)}{\lambda(e^{\lambda}+1)}\right] - R_S\left[1 - \frac{2(e^{\mu}-1)}{\mu(e^{\mu}+1)}\right]\right\} = 0. \quad (27)$$

It is noted that this equation can also be derived from equations (24) and (25) by a careful expansion for $\bar{v} \to 0$. Furthermore, for this case the perturbation distributions (22) and (23) reduce to those given by equation (26).

The characteristic equations for the stability parameter, σ, are equation (27) for the onset of motion from rest and equation (24) for the stability of the steady flow solutions. The nature of the stability is determined by the behaviour of σ. In the following both equations are solved by various methods to derive the stability chart of the double-diffusive thermosyphon.

4.2. *Stability associated with the onset of motion from rest*

There are two main types of perturbation growth associated with thermal or double-diffusive instabilities:

(a) Monotonic instability, where σ is real and the critical disturbance grows exponentially with time. This behaviour corresponds to the 'principle of exchange of stability' and on the marginal stability lines $\sigma = 0$.

(b) Oscillatory instability, where σ is complex, the critical perturbation growth is oscillatory and marginal stability is exhibited by steady oscillations, $\sigma = iw$ and the amplitude neither increases nor decays.

In the following we investigate the characteristic equation (27) to find marginal stability lines, $\mathrm{Re}(\sigma) = 0$, in the form of $R_T = R_T(R_S; q; P)$ and stability regions in the Rayleigh numbers plane R_S–R_T.

In previous stability analyses of the onset of motion in thermosyphons with a temperature gradient only [10, 16, 17] it was discovered that the instability associated with initiation of motion from rest is monotonic. We therefore start by trying the marginal solution $\sigma = 0$ for equation (27). Expanding this equation (with relations (26c)) for small real values of σ and approaching the limit $\sigma \to 0$, we obtain

$$R_T = 6 + qR_S \quad \text{monotonic marginal stability line (MMSL).} \quad (28)$$

Condition (28) holds for all values of q and R_S.

In ref. [10] it was found that the critical Rayleigh number for the onset of motion in a thermosyphon with no mass diffusion is $R_T = 6$. This result is obviously a special case of the more general condition (28), with $R_S = 0$. However, for the simple thermosyphons

treated in refs. [10, 16, 17] the critical Rayleigh numbers for marginal stability of the 'conductive solutions' coincide with the minimal R_T values for the existence of steady flow solutions, which also correspond to the limiting velocity $\bar{v} = 0$. In our case, a completely different behaviour is observed from the results of Section 3, see Figs. 2 and 3: for $q > 1$, $R_S > 0$ there exist steady flow solutions for thermal Rayleigh numbers, R_T, below the values given by equation (28) for which $\bar{v} = 0$. The critical R_T for a steady flow is given by $R_{Tc}(R_S; q)$, as in Figs. 2 and 3. These two lines, which are independent of the modified Prandtl number, P, are included in the complete stability charts for various values of q and P, Figs. 4–6.

We now return to the characteristic equation (27) and investigate it, looking for possible oscillatory instabilities of the rest state. In particular, it is interesting to find whether the critical line R_{Tc} is a marginal stability line. This investigation has been performed in two stages. The first consisted of using the Nyquist criterion in order to get a preliminary indication for the existence of oscillatory unstable disturbances. According to this method, cf. ref. [25], the complex function $Y_0(iw)$ is plotted for $-\infty < w < \infty$. If the curve for a given combination of R_T, R_S, q and P encircles the origin in the complex Y-plane, the state specified by these parameters is unstable.† The results of numerical calculations performed by this procedure showed that there are, indeed, oscillatory unstable rest states for various values of the system parameters. Moreover, such instabilities appear both below and above the line R_{Tc} in Figs. 4–6, which indicates that this line does not represent marginal stability of the rest state. In the second stage a method suggested by ref. [18] has been employed: equation (27) is rearranged in the form $R_T = \tilde{R}_T(iw; R_S, q, P)$, where $\tilde{R}_T$ is a complex function of w. At a point of marginal stability for some R_S, q and P, $\mathrm{Im}[\tilde{R}_T(w)] = 0$ because the parameter R_T is real. Thus by solving this equation we obtain the frequency, w, of the critical disturbance. This value of w is finally used to calculate $R_T = \mathrm{Re}[\tilde{R}_T(w)]$, giving a point on the marginal stability line for the specified parameters R_S, q and P.

The results are shown in the stability charts presented in Figs. 4–6 for three different values of the inverse Lewis number, q. Each chart in the plane of the saline and thermal Rayleigh numbers R_S, R_T includes three (solid) oscillatory marginal stability lines (OMSL) for three values of the modified Prandtl number, P. As can be seen, these are nearly straight lines; however, the numerical solution reveals that they curve, especially in the vicinity of the points where they branch off the monotonic marginal stability line (MMSL) given by equation (28). The bifurcation points are obtained from equation (27): the complex function $Y_0(iw)$ is expanded for small values of w and its limit for $w \to 0$ is sought. Two coupled equations are thus obtained, $\mathrm{Re}(Y_0) = \mathrm{Im}(Y_0) = 0$. One of them (the latter) obviously reduces to relation (28) (the point lies on this MMSL). The former equation, together with this relation, leads to the following expressions for the bifurcation points of the monotonic and oscillatory marginal stability lines:

$$R_S^* = \frac{6(1+10/P)}{q(q-1)}; \quad R_T^* = 6 + qR_S^*. \tag{29}$$

Table 1. Bifurcation points of the monotonic and oscillatory stability lines: values of the saline and thermal Rayleigh numbers, R_S^* and R_T^*, for various values of the inverse Lewis number, q, and the modified Prandtl number, P (see also Figs. 4–6).

q		P = 0.1	1	10
2	R_S^*	303	33	6
	R_T^*	612	72	18
10	R_S^*	6.733	0.733	0.133
	R_T^*	73.33	13.33	7.333
100	R_S^*	0.0612	0.00667	0.001212
	R_T^*	12.12	6.667	6.1212

Table 1 includes the coordinates of these points for all the values of q and P in Figs. 4–6.

It is noted that the most interesting stability phenomena occur in the first quadrant (positive R_T and R_S) of the charts in Figs. 4–6. As shown in the figures, the MMSL extends into the third quadrant. Any state (point) above it, including the whole second quadrant, is unstable. The entire fourth quadrant lies in the stability zone.

The stability charts presented in Figs. 4–6 depict several interesting phenomena. The most 'peculiar' behaviour is that the oscillatory marginal stability lines intersect the critical line, R_{Tc}, for existence of a steady flow solution. There is no such solution below the line R_{Tc}, while the stable region (for small disturbances) for any value of P lies below the corresponding OMSL. Thus for any point (state) located in a region such as I in Fig. 5 (for $q = 10$, $P = 0.1$), there are steady flow solutions inside the domain of linear stability. This is referred to as a region of subcritical instability, and was discovered also by the analysis of ref. [6] (neglecting thermal and mass diffusivities). The implication of the existence of this phenomenon is that while the linear stability predicts a decay of any disturbance, there are some perturbations that do grow, and only a more exact nonlinear model would be capable of tracing them.

Let us examine now the states represented by points in a region such as II in Fig. 5 (for $q = 10$ and $P = 0.1$, again). Although they are linearly unstable, no steady flow solutions are established for the parameters defining them. This indicates that a small disturbance would initially grow, but then non-linear effects inter-

† It is noted that Y_0, defined in equation (27), does not have any pole in the half plane $\mathrm{Re}(\sigma) \geq 0$ (including the point $\sigma = 0$, which has already been treated above).

fere, leading to either a decay to the rest state or to a transient behaviour, possibly of a 'chaotic' type. As mentioned above, the latter has been predicted for thermosyphons [11–13], and for a loop with the Soret effect [8]. It is noted that a region of this type is not found by the simplified model of ref. [6]. Furthermore, a non-linear analysis was used in ref. [6] to show that in the linearly stable region where steady flow solutions do not exist (equivalent to the domain below both R_{Tc} and OMSL in our case), all the solutions decay, i.e. it is a region of global stability. This non-linear analysis was not carried on in ref. [6] to investigate the region of type I in Fig. 5. Such an analysis is beyond the scope of the present study and is left for future work.

A complete description of the stability charts in Figs. 4–6 is given in Section 5.

4.3. *Stability of the steady flow solutions*

The stable nature of the steady flow solutions is determined by the characteristic equation (24). We check, first, whether there are any monotonic instabilities of the steady-state flows. For this, expressions F and G in equation (25) are expanded for small real values of σ, and the limit $\sigma \to 0$ is approached, to yield

$$F^\circ \equiv F|_{\sigma=0} = \left[\frac{1}{v} - \frac{v\,e^v}{(e^v-1)^2}\right] \tag{30a}$$

$$G^\circ \equiv G|_{\sigma=0} = \frac{1}{v}\left[\frac{1}{qv} - \frac{qv\,e^{qv}}{(e^{qv}-1)^2}\right]. \tag{30b}$$

The velocity, v, in these relations is the solution of equation (14). We therefore introduce $R_T(v; R_S, q)$ from equation (14), F° and G° from equation (30) and $\sigma = 0$ into equation (24). The resulting relationship between R_S, q and v obtained in this way is exactly equation (15), which together with equation (14) define the critical line R_{Tc}. This is the critical line for the thermal Rayleigh number below which there does not exist any steady flow solution and it also separates the double steady solutions, see Figs. 2 and 3. Thus the critical line R_{Tc}, in addition, is a monotonic marginal stability line for the steady flow solutions.

The Nyquist criterion (Section 4.2) has been used to find the stability regimes of the steady flows, in the stability charts of the Rayleigh numbers plane, Figs. 4–6. The results of the numerical computations show that in the range of double solutions (between the lines MMSL and R_{Tc} in Figs. 4–6), all the steady flows with the lower velocity—below the lines R_{Tc} in Figs. 2 and 3, are unstable,† while all the flows with the higher velocity (above the lines R_{Tc}) are stable. In the range where a single steady solution exists, i.e. above the lines MMSL in Figs. 4–6, the solution is stable. Furthermore, the results obtained by the numerical calculations based on the Nyquist method show that there does not exist any oscillatory instability in the whole domain of the system parameters R_T, R_S, q and P. This result may seem rather surprising at first glance, because it is well known that steady flow solutions of thermosyphons are unstable in some range of system parameters. However, as shown in ref. [16] for a loop with a temperature gradient only, the solution for small thermal conduction (high values of R_T) corresponds to the low-velocity stable region found by Welander [26] for the vertical thermosyphon. A finite conductivity or thermal and mass diffusivities are stabilizing factors, thus the steady solutions of the loop under consideration are stable as indicated above.

It is noted that the result obtained here, that the flow with lower velocity in the case of multiple steady flow solutions is unstable, is not general. In other thermosyphons where multiple solutions have been observed [20–23], there is no general rule for stability. All the solutions or some of them can be stable or unstable and the instabilities are always of the oscillatory type, as in loops with a temperature gradient only, cf. ref. [10]. Here the marginal stability line is for monotonic growth of the disturbances.

In the system treated here, the side walls were assumed to be insulated. The effects of transverse heat and mass fluxes have been investigated for the toroidal loop in refs. [6, 7, 11–13] (without axial conduction and diffusion), in ref. [8] without axial conduction but with axial diffusion, including the Soret effect, and finally in ref. [17] with thermal conduction. As pointed out in ref. [17], the Rayleigh numbers defined in these previous studies are based on transverse heat and mass convection coefficients. When axial diffusions are considered the effects of these coefficients are expressed by Biot numbers, *Bi*. It is shown, indeed, in ref. [17] that the results of ref. [12], for example, are the asymptotic expansions for large Rayleigh and Biot numbers. In the range of small R and Bi an interesting phenomenon has been obtained in ref. [17], namely a minimum for the function of the critical Rayleigh number, R_T (Bi), for the onset of motion. From this we can also learn about the possible effects of transverse heat fluxes in the system considered here. If the heat convection coefficient is small and increasing from zero, the critical Rayleigh number of the rest state would decrease, because of the increase of the driving force caused by heating or cooling from the side. When this coefficient becomes large, the temperature variations around the loop tend to smooth out, causing a decrease of the driving force and an increase of the critical Rayleigh number. Thus a minimum for the curve of the latter as a function of the Biot number is expected here too.

5. SUMMARY

Several types of instabilities have been discovered by the theoretical analysis of the double-diffusive thermosyphon shown in Fig. 1 : those associated with the onset of motion and others involving multiple steady flow solutions (see Figs. 2 and 3) and their stability.

† In ref. [7] it is merely hinted that such a solution is 'expected to be unstable'.

The method to derive the complete linear stability chart, including all these phenomena, is described in Sections 3 and 4. Here we summarize the results shown in Figs. 4–6, which include the charts in the Rayleigh numbers plane R_S–R_T for three values of the inverse Lewis number, q and for various modified Prandtl numbers, P.

(a) Instabilities of the 'conductive solution', i.e. associated with the onset of motion from rest.

The line $R_T = 6 + qR_S$ is a monotonic marginal stability line (MMSL); every point (representing a state with the respective values of the parameters) above it is unstable, with a monotonically growing disturbance. The line is the true stability boundary for $R_S \leqslant R_S^*(q, P)$, see Figs. 4 and 5 for example. In the range $R_S \geqslant R_S^*$ the true stability boundary for every value of P is represented by the corresponding OMSL (see Fig. 4). In this range MMSL is still a critical line for monotonic perturbations, but the most dangerous disturbance is an oscillatory one and the stability margin is on OMSL, which lies below MMSL. The 'conductive solution' is linearly unstable for any state above the former.

The OMSL curves intersect the line R_{Tc}, marking the condition for existence of steady flow solutions. In the region of subcritical instability, e.g. I in Fig. 5, steady flows are established although the rest state is linearly stable. In the unstable region above OMSL and below R_{Tc}, e.g. II in Fig. 5, no 'convective solutions' exist. Both phenomena are due to non-linear effects, not considered here.

(b) Instabilities of the 'convective solutions'.

There are no steady flow solutions in the region below the line R_{Tc} in the stability chart, see Figs. 4–6. It is noted that for $R_S < 0$ R_{Tc} coincides with the line $R_T = 6 + qR_S$. Two steady flow solutions exist in the region between these two lines, see also Figs. 2 and 3. The solution with the lower velocity is always monotonically unstable, (to small perturbations) thus the curve R_{Tc} is also a marginal stability line. All the steady 'convective solutions' represented by points above R_{Tc} are stable, including the higher velocity one in the region of double solutions, and the single solution above the line $R_T = 6 + qR_S$.

It is noted that the trivial 'conductive solution' always exists, together with the 'convective solution' (or solutions), and its stability was discussed above. In addition, all the steady flow solutions are actually pairs of solutions, because there is no preferred flow direction in the loop.

Acknowledgement—This work was supported by the Technion V.P.R. Fund–B. & N. Ginsburg Energy Research Fund. Their help is greatly appreciated.

REFERENCES

1. Y. Zvirin, A review of natural circulation loops in pressurized water reactors and other systems, *Nucl. Engng Des.* **67,** 203–225 (1981).
2. A. Mertol and R. Greif, A review of natural circulation loops, NATO Advanced Study Inst. on Natural Convection, Izmir, Turkey, July 16–27 (1984). Also in *Natural Convection: Fundamentals and Applications* (Edited by W. Aung, S. Kakac and R. Viskanta). Hemisphere, New York (1985).
3. P. F. Linden, Salt fingers in a steady shear flow, *Geophys. Fluid Dynamics* **6,** 1–27 (1974).
4. M. Magen, D. Pnueli and Y. Zvirin, The stability chart of parallel shear flows with double-diffusive processes—general properties, *J. Engng Math.* **19,** 175–187 (1985).
5. M. Magen, D. Pnueli and Y. Zvirin, The stability chart of double diffusive processes with parallel flows—construction by the Galerkin and continuation methods, *J. Engng Math.* **20,** 127–144 (1986).
6. W. L. Siegmann and L. A. Rubenfeld, A nonlinear model for double-diffusive convection, *SIAM J. Appl. Math.* **29,** 540–557 (1975).
7. L. A. Rubenfeld and W. L. Siegmann, Nonlinear dynamic theory for a double-diffusive convection model, *SIAM J. Appl. Math.* **32,** 871–894 (1977).
8. J. E. Hart, A model of flow in a closed-loop thermosyphon including the Soret effect, *J. Heat Transfer* **107,** 840–849 (1985).
9. Y. Zvirin, A natural circulation loop with double diffusive processes—steady flow and the onset of motion, *Proc. 8th Int. Heat Transfer Conf.*, San Francisco, California, Vol. 4, pp. 1551–1556 (1986).
10. Y. Zvirin, The instability associated with the onset of motion in a thermosyphon, *Int. J. Heat Mass Transfer* **28,** 2105–2111 (1985).
11. M. Sen, E. Ramos and C. Treviño, The toroidal loop with known heat flux, *Int. J. Heat Mass Transfer* **28,** 219–233 (1985).
12. J. E. Hart, A new analysis of a closed loop thermosyphon, *Int. J. Heat Mass Transfer* **27,** 125–136 (1984).
13. J. A. Yorke and E. D. Yorke, Chaotic behavior and fluid dynamics. In *Topics in Applied Physics, Hydrodynamic Instabilities and the Transition to Turbulence* (Edited by H. L. Swinney and J. P. Gollub), Chap. 4. Springer, Berlin (1981).
14. K. E. Torrance and V. W. L. Chan, Heat transfer by a free-convection loop embedded in a heat conducting solid, *Int. J. Heat Mass Transfer* **23,** 1091–1097 (1980).
15. H. H. Bau and K. E. Torrance, Transient and steady behavior of an open symmetrically-heated free convection loop, *Int. J. Heat Mass Transfer* **24,** 597–609 (1981).
16. Y. Zvirin, The onset of flows and instabilities in a thermosyphon with parallel loops, *Nucl. Engng Des.* **92,** 217–226 (1986).
17. Y. Zvirin, The onset of motion in a toroidal thermosyphon, *J. Engng Math.* **20,** 3–20 (1986).
18. A. Ronen and Y. Zvirin, The behavior of a toroidal thermosyphon at high Graetz (and Grashof) numbers, *J. Heat Transfer* **107,** 254–258 (1985).
19. A. Mertol, R. Greif and Y. Zvirin, Two dimensional study of heat transfer and fluid flow in a natural circulation loop, *J. Heat Transfer* **104,** 508–514 (1982).
20. J. C. Chato, Natural convection flows in parallel-channel systems, *J. Heat Transfer* **85,** 339–345 (1963).
21. Y. Zvirin, The effects of a throughflow on the steady state and stability of a natural circulation loop, AIChE Symposium Series, 19th National Heat Transfer Conference, Orlando, Florida, pp. 238–249 (1981).
22. A. Mertol, R. Greif and Y. Zvirin, The transient, steady-state and stability behavior of a natural convection loop with a throughflow, *Int. J. Heat Mass Transfer* **24,** 621–633 (1981).
23. P. R. Jeuck, III, L. Lennert and R. L. Kiang, Single-phase natural circulation experiments on small break accident heat removal, EPRI Reports NP-2006, NP-81-18-LD (August 1981).

24. Y. Zvirin, P. R. Jeuck, III, C. W. Sullivan and R. B. Duffey, Experimental and analytical investigation of a natural circulation system with parallel loops, *J. Heat Transfer* **103,** 645–652 (1981).
25. H. F. Creveling, J. F. DePaz, J. Y. Baladi and R. J. Schoenhals, Stability characteristics of a single-phase free convection loop, *J. Fluid Mech.* **57,** 65–84 (1975).
26. P. Welander, On the oscillatory instability of a differentially heated fluid loop, *J. Fluid Mech.* **29,** 17–30 (1966).

INSTABILITES DANS UN THERMOSIPHON DOUBLEMENT DIFFUSIF

Résumé—On étudie le comportement stationnaire et la stabilité d'une boucle de circulation naturelle doublement diffusive. Dans le thermosiphon constitué par deux canaux verticaux, le fluide est soumis à des gradients de température et de salinité. Les équations de continuité, de quantité de mouvement, d'énergie et de diffusion de masse sont écrites pour un modèle unidirectionnel et un écoulement laminaire. Les solutions permanentes incluent le cas trivial "conductif" sans vitesse dans la boucle ($v = 0$) et les solutions de convection lorsque le nombre de Rayleigh thermique R_T dépasse une valeur critique R_{Tc} qui dépend du nombre de Rayleigh de salinité R_S et du nombre inverse de Lewis q. Dans un certain domaine des paramètres du système, les "solutions de convection double" sont obtenues. Les résultats de l'analyse de stabilité linéaire montrent que ceux pour v plus faible sont toujours instables et que les autres sont stables. Le graphe de stabilité, dans le plan $R_S - R_T$, obtenu par cette analyse, concerne aussi une description des instabilités associées avec la mise en mouvement depuis le repos. Les frontières de stabilité marginale monotone (MMSL) $R_T = 6 + qR_S$, celles oscillatoires (OMSL) qui dépendent aussi du nombre de Prandtl et bifurquent à partir de MMSL. Un phénomène intéressant, montré par la solution, est que OMSL coupe la courbe R_{Tc}, représentant les conditions critiques pour l'existence de solutions permanentes.

INSTABILITÄTEN IN EINEM DURCH TEMPERATUR- UND KONZENTRATIONSUNTERSCHIEDE BETRIEBENEN THERMOSYPHON

Zusammenfassung—Der stationäre Zustand und das Stabilitätsverhalten eines Naturumlaufs wurden theoretisch untersucht. Das Fluid in dem aus zwei vertikalen Kanälen bestehenden Thermosyphon unterliegt sowohl einem Temperatur- als auch einem Salzgehaltsgradienten. Die Erhaltungsgleichungen für Masse, Impuls, Energie und Stofftransport wurden auf der Grundlage eines eindimensionalen Modells für laminare Strömung aufgestellt. Die Lösungen für den stationären Fall beinhalten den trivialen Fall der Wärmeleitung bei der Strömungsgeschwindigkeit $v = 0$ und Ergebnisse für konvektive Strömung, wenn nämlich die thermische Rayleigh-Zahl R_T einen kritischen Wert R_{Tc} überschreitet, der von der Salzgehalts-Rayleigh-Zahl R_S und der inversen Lewis-Zahl q abhängt. In einem bestimmten Bereich der Systemparameter erhält man für den konvektiven Fall zweifache Lösungen. Die Ergebnisse der linearen Stabilitätsanalyse zeigen, daß die Lösung mit der niedrigeren Geschwindigkeit immer instabil und alle anderen Lösungen für stationäre Strömung stabil sind. Das von dieser Untersuchung abgeleitete Stabilitätsschaubild in der R_S–R_T-Ebene enthält außerdem eine Beschreibung der mit dem Einsetzen der Bewegung aus dem Ruhezustand verbundenen Instabilität. Die Stabilitätsgrenzen beinhalten die momentanen Stabilitätslinien (MMSL) $R_T = 6 + qR_S$ und die Stabilitätslinien für Oszillation (OMSL), die außerdem von der Prandtl-Zahl abhängen und von der MMSL aufgespalten werden. Ein durch die Lösung dargelegtes interessantes Phänomen ist, daß OMSL die Linie R_{Tc} schneidet, welche letztere die kritischen Bedingungen für die Existenz der Lösungen einer stationären Strömung darstellt.

НЕУСТОЙЧИВОСТИ В ТЕРМОСИФОНЕ С ДВОЙНОЙ ДИФФУЗИЕЙ

Аннотация—Теоретически изучаются стационарные решения и их устойчивость в задачах для контура с двойной диффузией. На жидкость в термосифоне, состоящем из двух вертикальных каналов, воздействует как температурный градиент, так и градиент солености. Определяющие уравнения неразрывности, движения, энергии и диффузии записаны на основе одномерной модели для ламинарного течения. Стационарные решения включают как тривиальное «кондуктивное» решение–для случая отсутствия потока в контуре, $v = 0$, так и для «конвективного» течения, когда тепловое число Рэлея R_T превышает его критическое значение R_{Tc}, зависящее от числа Рэлея солености R_S и обратного числа Льюиса q. В некотором диапазоне параметров системы получены двойные «конвективные» решения. Результаты анализа по линейной теории устойчивости показывают, что течения с меньшим v всегда неустойчивы, а все остальные стационарные решения являются устойчивыми. Кривая устойчивости в плоскости $R_S - R_T$, полученная с помощью этого анализа, кроме того включает описание неустойчивостей, связанных с возникновением движения из состояния покоя. Границы маргинальной устойчивости включают линии монотонной маргинальной устойчивости (ЛММУ) $R_T = 6 + qR_S$ и осцилляционной маргинальной устойчивости (ЛОМУ), которые зависят от числа Прандтля и ответвляются от ЛММУ. Интересные эффекты, вытекающие из решения, состоят в том, что ЛОМУ пересекает линию R_{Tc}, представляя собой критические условия существования для стационарных течений.